CSIRO PUBLISHING

COLLECTION | RESEARCH PAPER
https://doi.org/10.1071/CH25079

AUSTRALIAN JOURNAL OF CHEMISTRY

The C-terminal region of *Opisthorchis viverrini* granulin-1 promotes cell proliferation in the absence of regular secondary structure

Mohadeseh Dastpeyman[A,B], David T. Wilson[A], Alex Loukas[A], Michael J. Smout[A,*] and Norelle L. Daly[A,*]

For full list of author affiliations and declarations see end of paper

***Correspondence to:**
Michael J. Smout
Australian Institute of Tropical Health and Medicine, James Cook University, Cairns, Qld, Australia
Email: michael.smout@jcu.edu.au

Norelle L. Daly
Australian Institute of Tropical Health and Medicine, James Cook University, Cairns, Qld, Australia
Email: norelle.daly@jcu.edu.au

Handling Editor:
Mibel Aguilar

Received: 14 May 2025
Accepted: 3 October 2025
Published: 17 November 2025

Cite this: Dastpeyman M *et al.* (2025) The C-terminal region of *Opisthorchis viverrini* granulin-1 promotes cell proliferation in the absence of regular secondary structure. *Australian Journal of Chemistry* **78**, CH25079. doi:10.1071/CH25079

© 2025 The Author(s) (or their employer(s)). Published by CSIRO Publishing.
This is an open access article distributed under the Creative Commons Attribution-NonCommercial-NoDerivatives 4.0 International License (CC BY-NC-ND)

OPEN ACCESS

ABSTRACT

Topical application of granulin-derived peptides has the potential to alleviate the burden of chronic wounds. Granulins are a family of growth factor proteins that generally contain six disulfide bonds and are found in most organisms. They have diverse sequences and complex structure–function relationships. Select examples are potent wound healing agents, making it important to improve our understanding of how granulins fold and the structural features critical for bioactivity. We have previously shown that fragments corresponding to the N-terminal region of the parasite granulin, *Ov*-GRN-1, can fold autonomously even with a non-native disulfide bond and still have well-defined structures. Here, we show that this phenomenon appears unique to the N-terminal region, as a peptide corresponding to the C-terminal fragment of *Ov*-GRN-1 does not fold independently in an analogous manner to the N-terminal region. Despite a lack of structure in the C-terminal granulin fragment, this peptide promotes cell proliferation, indicating that the sequence might be more important than the three-dimensional structure for *Ov*-GRN-1 wound-healing bioactivity.

Keywords: disulfide-rich peptides, disulfide-rich peptide scaffolds, granulin cysteine motif, minimising proteins, peptide NMR, peptide therapeutics, unstructured peptides, wound healing.

Introduction

Wound healing is a complex process and when the multiple factors involved fail to effectively integrate, chronic wounds can result.[1,2] A range of peptides and proteins have been shown to promote wound healing properties,[3] including progranulin proteins.[4,5] Progranulin is a multifunctional protein belonging to the growth factor protein family[6] and is involved in diverse biological activities in addition to wound healing, such as carcinogenesis,[5] regeneration and inflammation.[7,8]

The human progranulin comprises seven-and-a-half repeats, which are cleaved to produce individual granulin peptides. Granulins share a highly conserved cysteine-rich framework; however, the bioactivities of the different isoforms vary and in some cases, are distinct from those of the precursor protein,[9] thereby complicating their structure–function relationships.[6,10] Despite their biological importance, the biochemical and functional characterisation of individual human granulin peptides remains limited, mainly due to the difficulties associated with large-scale purification of endogenous proteins or production of structurally well-defined proteins.[9]

Over the past decade, advances in the study of granulin peptides isolated from species other than humans, including carp,[11] zebrafish[12] and liver-fluke,[13] have significantly enhanced our understanding of their folding properties, structural features and structure–function relationships. The three-dimensional structures of carp granulin-1 and zebrafish granulin AaE are well-defined with a laddered arrangement of the six disulfide bonds and stacking of four β-hairpins (Fig. 1).[10,12,14] However, not all granulin modules have well defined structures, with human granulin A (hGRN2), human granulin

Collection: 70th Birthday Tribute to Professor David Craik

Downloaded from connectsci.au/ch/article-pdf/doi/10.1071/CH25079/1798680/ch25079.pdf by James Cook University user on 29 October 2026

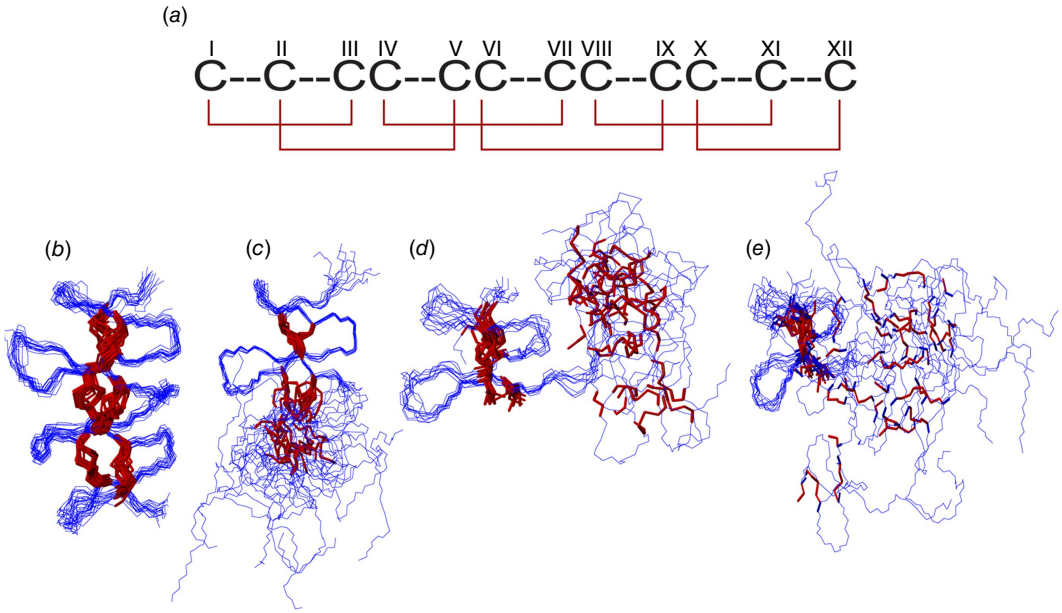


Fig. 1. Granulin cysteine framework. (*a*) Schematic representation of the highly conserved cysteine framework and disulfide bond pairing present in the granulin family; the cysteine residues are numbered using Roman numerals (I–XII). Three-dimensional structure of (*b*) zebrafish granulin AaE (PDB ID: 6CKU),[12] (*c*) hGRN A (PDB ID: 2JYE),[9] (*d*) hGRN C isomer 1 (PDB ID: 2JYT),[9] (*e*) hGRN C isomer 2 (PDB ID: 2JYU).[9]

C (hGRN5) and several of the zebrafish granulin domains having varying degrees of structural disorder, particularly in the C-terminal domain (Fig. 1*b–e*).[9,12,14,15]

Liver-fluke granulin, *Ov*-GRN-1, is the main growth factor isolated from the excretory or secretory product of the liver fluke *Opisthorchis viverrini*.[16] Recombinant *Ov*-GRN-1 significantly induces human fibroblast cell proliferation and accelerates wound repair in a mouse model, but is difficult to make in high yields.[13] Hence, we investigated the design and characterisation of downsized analogues.[17,18]

We previously demonstrated that a peptide corresponding to the N-terminal half of *Ov*-GRN-1, comprising the first six cysteine residues of the full domain, named *Ov*-GRN$_{12_35_3s}$, can fold autonomously with three disulfide bonds (Fig. 2) and display potent wound healing properties similar to the full-length *Ov*-GRN-1.[17] The sequences of full-length *Ov*-GRN-1 and *Ov*-GRN$_{12_35_3s}$ are given in Table 1. Investigation into the structure-function relationships of the N-terminal region of *Ov*-GRN-1 led to the development of a truncated analogue with improved oxidation yield and wound healing properties.[18] Our previous studies also demonstrated that the disulfide bond between CysIV and CysVI, which is not present in the characteristic granulin disulfide bond pairing pattern, has an important role in maintaining a well-defined β-hairpin structure of the truncated analogues, as well as its bioactivity (Fig. 2).[17–20]

Autonomous folding of a disulfide-rich peptide into a well-defined structure with potent bioactivity is a significant advantage for the potential pharmaceutical development of *Ov*-GRN-1 derived compounds, as regioselective oxidation

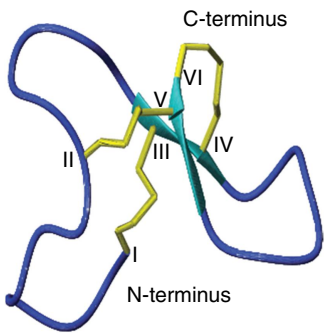


Fig. 2. Three-dimensional structure of *Ov*-GRN$_{12–35_3s}$ (PDB ID: 5UJG), previously described.[17,18] Ribbon representations are of the lowest energy structures from ensembles of 20 structures. Disulfide bonds are shown as yellow sticks and only the backbone atoms are displayed. The Figure was prepared using *MOLMOL* (ver. 1.0.7, see https://sourceforge.net/p/molmol/wiki/Home/).[26]

of disulfide-rich peptide-based therapeutics is costly, laborious and complicated in large-scale manufacturing.[21–25]

Despite the interesting potential associated with the N-terminal region, the C-terminal half of granulin domains has not been studied in isolation. In the current study, we show for the first time that a peptide corresponding to the C-terminal region of *Ov*-GRN-1 comprising six cysteine residues appears unstructured following *in vitro* folding, but still displays bioactivity.[18] Providing insights into the folding of the granulin structural motif further enhances our fundamental understanding of protein folding as well as the potential of granulins as wound-healing agents.

Downloaded from connectsci.au/ch/article-pdf/doi/10.1071/CH25079/1798680/ch25079.pdf by James Cook University user on 29 October 2026

Results and discussion

Peptide synthesis and oxidation

To determine if the C-terminal half of *Ov*-GRN-1 can fold independently with three disulfide bonds, we synthesised a peptide corresponding to residues 39–66 of the *Ov*-GRN-1 protein (called *Ov*-GRN$_{39–66_3s}$), which spans the region encompassing CysVII to CysXII (Table 1). For comparison, a peptide corresponding to residues 9–35 (*Ov-GRN*$_{9–35_3s}$) and spanning the region that includes CysI to CysVI, was also synthesised. Both peptides contain at least three residues prior to the first cysteine residue.

Peptides were synthesised using Fmoc solid-phase peptide synthesis on 2-chlorotrityl resin and the disulfide bonds formed by air oxidation in ammonium bicarbonate (0.1 M) and glutathione (5 mM) at room temperature. These oxidation conditions were chosen based on the previous studies on *Ov*-GRN-1 truncated peptides.[17–19] The analytical RP-HPLC traces of the oxidation reactions for *Ov*-GRN$_{9–35_3s}$ contain a relatively sharp peak that eluted earlier than the other peaks (Supplementary Fig. S1). The folding profile was consistent with our previous studies on *Ov*-GRN-1 N-terminally truncated peptides[17,18] and with studies carried out in other laboratories, including carp granulin 1 and 2,[27] human granulin domains[9] and recombinant zebra fish granulins expressed in *E. coli* (DE3),[12] which indicated that the early eluting peak was likely to have a well-folded structure. The relative folding yield, calculated based on the area of the early-eluting peak relative to the total peak area, was determined to be 43% for *Ov*-GRN$_{9–35_3s}$ The early-eluting peak was purified by semi-preparative RP-HPLC.

The RP-HPLC trace for the oxidation of the C-terminal truncated peptide, *Ov*-GRN$_{39–66_3s}$, contained numerous poorly resolved peaks (Fig. 3), in contrast to the N-terminal truncated

Table 1. Sequences of granulin peptides.

Peptide	Sequence
Ov-GRN-1[A]	...DTLQPIRSPS**C**PDPVYT**C**RPGQT**CC**RGLHGYG**CC**PMDSAT**CC**SDLLH**CC**PHGTA**C**TAYGL**C**VRGD...
Ov-GRN$_{12_35_3s}$[B]	**C**PDPVYT<u>**C**RPGQT**CC**</u>RGLHGYG**CC**
Ov-GRN$_{9_35_3s}$	SPSCPDPVYT<u>C</u>RPGQT<u>C</u>CRGLHGYGCC
Ov-GRN$_{39–66_3s}$	SAT**CC**SDLLH**CC**PHGTA**C**TAYGL**C**VRGD

The ellipses (...) indicate a sequence gap. Cysteine residues are shown in bold to indicate granulin cysteine motif.
[A]Residues 20–84 of the *Ov*-GRN-1 sequence are shown in this table.
[B]The sequence of the previously studied, *Ov*-GRN$_{12_35_3s}$,[17] is cited accordingly and presented in this table for comparison purposes. Inter-cysteine loop 2 (GRN-L2), previously published,[19] is underlined.

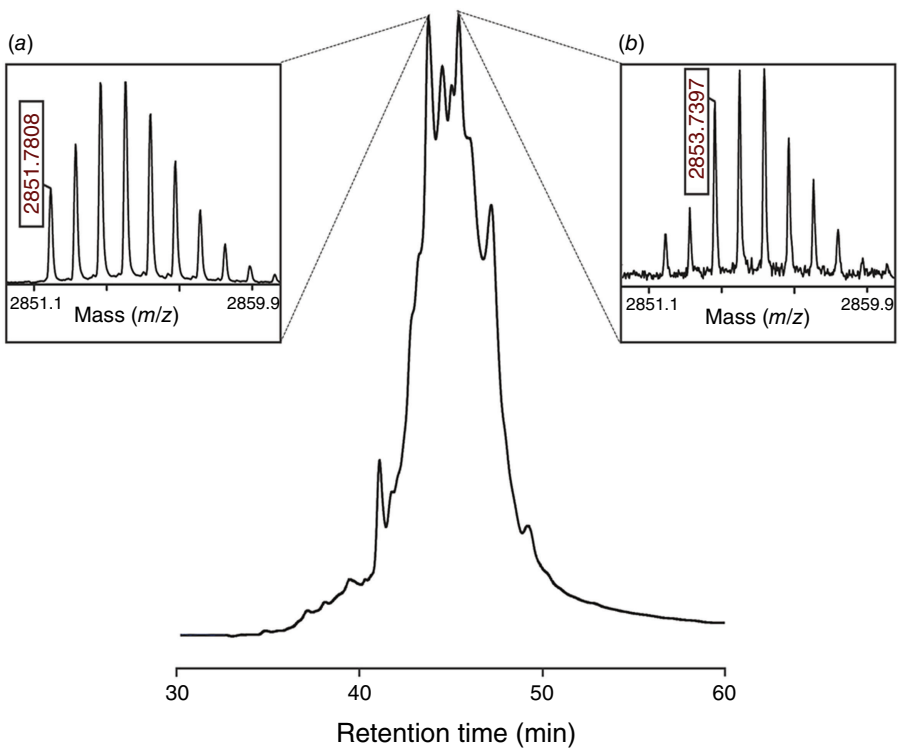


Fig. 3. RP-HPLC and mass analysis of the *Ov*-GRN$_{39–66_3s}$ oxidation reaction. The oxidation mixture was fractionated using a C_{18} preparative RP-HPLC column following 82 h of oxidation. The separation method was as follows: a gradient of 0–50% solvent B over 50 min with a flow rate of 6 mL min^{-1}. Fractions were collected and the peptide mass was analysed using a SCIEX 5800 MALDI TOF/TOF spectrometer. The masses of different *Ov*–GRN$_{39–66_3s}$ disulfide bond isomers eluting at different time points are shown in boxes *a* and *b*. (*a*) Box *a* shows the ($(M + H)^+$ charged ion at *m/z* = 2851.7808), which corresponds to fully oxidised *Ov*-GRN$_{39–66_3s}$. (*b*) Box *b* shows the ($(M + H)^+$ charged ion at *m/z* = 2853.7397), which corresponds to the partially oxidised *Ov*-GRN$_{39–66_3s}$ with two disulfide bonds. The non-symmetric isotope pattern in box *b* indicates the presence of some traces of fully oxidised product from adjacent peaks.

Downloaded from connectsci.au/ch/article-pdf/doi/10.1071/CH25079/1798680/ch25079.pdf by James Cook University user on 29 October 2026

analogues of *Ov*-GRN-1 peptides, including *Ov*-GRN$_{9–35_3s}$, which exhibited an early-eluting peak corresponding to the fully oxidised species. Notably, no predominant peak was observed in the *Ov*-GRN$_{39–66_3s}$ oxidation mixture, even after extending the oxidation reaction to 82 h. Mass spectrometry analysis of the collected peaks at different time points revealed that some fractions corresponded to fully oxidised species, whereas some represented partially oxidised forms (Fig. 3).

As illustrated in Fig. 3, the cluster of poorly resolved peaks indicates the presence of analytes with highly similar biochemical properties that partially co-elute across adjacent peaks. This overlap prevented separation and characterisation of the fully oxidised species. To address this issue, we collected the apex of the peak appearing at the retention time of 43.1 min, which corresponded to the molecular weight of the fully oxidised species, and subjected it to repeated purification. Despite this repeated purification, there were still several overlapping peaks as shown in Supplementary Fig. S2. Given their identical mass, these peaks likely represent species with alternative disulfide bond arrangements, which could not be resolved chromatographically. This fraction was subsequently used for downstream analyses, including NMR spectroscopy and proliferation assays.

Folding of *Ov*-GRN$_{39–66_3s}$

Oxidative folding of disulfide-rich peptides *in vitro* can be significantly influenced by the folding conditions. For example, organic solvents such as isopropanol or acetonitrile can improve the folding efficiency of hydrophobic peptides by protecting the peptide from aggregation and possibly by additional stabilisation of the native conformation.[28,29] Positive effects of organic solvents were previously observed in the oxidative folding of hydrophobic conotoxins and the prototypic cyclotide kalata B1.[30] Comparison of the sequences of *Ov*-GRN$_{39–66_3s}$ and *Ov*-GRN$_{9–35_3s}$, with the Expasy *ProtParam* tool (see https://web.expasy.org/protparam/), indicates that *Ov*-GRN$_{39–66_3s}$ contains a higher proportion of hydrophobic residues compared to *Ov*-GRN$_{9–35_3s}$ (Table 2). However, the addition of acetonitrile and isopropanol into the folding mixture had no significant effect on the RP-HPLC profile for *Ov*-GRN$_{39–66_3s}$ folding (data not shown).

Table 2. Physicochemical characterisation of *Ov*-GRN-1 N-terminal and C-terminal analogues.

Peptide	Number of residues	pI	Aliphatic index	GRAVY
Ov-GRN$_{9–35_3s}$	27	7.56	25.19	-0.363
Ov-GRN$_{39–66_3s}$	28	5.92	62.86	0.368

pI is the abbreviation for the theoretical isoelectric point. Aliphatic index is defined as the relative volume of a protein occupied by amino acids with aliphatic side chains. Grand Average of Hydropathicity (GRAVY) score is calculated as the sum of hydropathy values of each amino acid residues, divided by the number of residues in the sequence. Positive GRAVY value refers to the hydrophobicity of a peptide and a negative value indicates hydrophilicity.

Significant differences in physicochemical properties of the N- and C-terminal truncated analogues of *Ov*-GRN-1 may contribute to their distinct folding behaviours. However, differences in folding properties could also be related to the cysteine framework itself. Notably, the highly conserved cysteine spacing is inverted in the C-terminal half of the molecule relative to the N-terminal region, as shown for *Ov*-GRN-1 in Table 1. It might not be energetically favourable for the C-terminal region of the granulin motif to fold with three disulfide bonds, given that the C-terminal region is reported to be disordered in several granulins (Fig. 1). Furthermore, the N-terminal half of granulins exists in nature as a discrete peptide, termed paragranulin,[6] whereas this is not the case for the C-terminal half. This distinction is likely to be the most telling factor contributing to the differences in folding between the N- and C-terminal regions of the *Ov*-GRN-1 granulin motif.

Overall, these results indicate that it is not energetically favourable for the C-terminal truncated analogue to fold autonomously, in the same way as the N-terminal analogues under the conditions used in this study. Regioselective disulfide bond formation is not investigated in this paper, given that the purpose of the study was to explore the autonomous folding of the *Ov*-GRN-1 C-terminal fragment spanning the second half of the granulin motif compared to the N-terminal fragment.

Structural analysis

One-dimensional proton spectra can provide insight into the type of secondary structure present in peptides and proteins.[31] The ^{1}H NMR spectrum of the *Ov*-GRN$_{39–66_3s}$ fully oxidised fraction had broad peaks with limited dispersion in the amide region (Fig. 4), indicating the peptide does not have a well-defined structure. By contrast, *Ov*-GRN$_{9–35_3s}$ showed large chemical shift dispersion in the amide region (Fig. 4), consistent with peptides containing β-sheet structure. In our previous

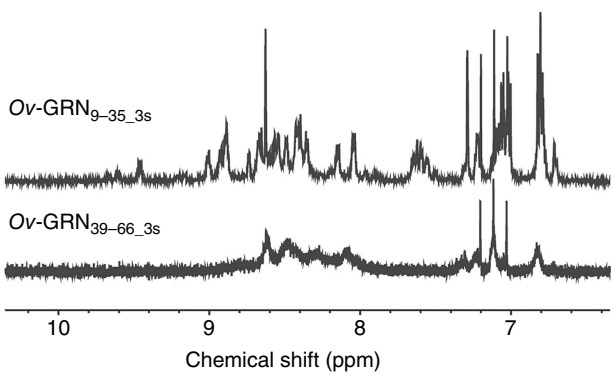


Fig. 4. One-dimensional proton NMR spectra for truncated granulin analogues. Spectra are shown from 6 to 10.5 ppm; this region primarily contains the amide protons. *Ov*-GRN$_{9–35_3s}$ has significant chemical shift dispersion in this region compared to the limited dispersion for *Ov*-GRN$_{39–66_3s}$.

Downloaded from connectsci.au/ch/article-pdf/doi/10.1071/CH25079/1798680/ch25079.pdf by James Cook University user on 29 October 2026

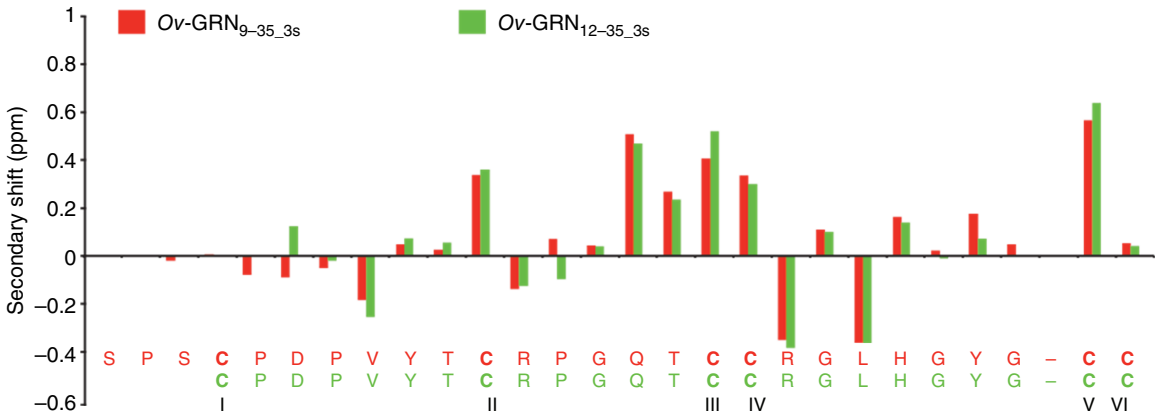


Fig. 5. αH Secondary-shift comparison for truncated analogues from the N-terminal domain of *Ov*-GRN1. The αH secondary shifts were calculated by subtracting the random coil ^{1}H NMR chemical shifts previously reported by Wishart *et al.*[32] from the experimental αH chemical shifts. The colour used for each peptide is shown at the top of the diagram. The sequences of *Ov*-GRN$_{12–35_3s}$ (green) and *Ov*-GRN$_{9–35_3s}$ (red) are given at the bottom of the diagram.

study, we showed that the structure of *Ov*-GRN$_{12–35_3s}$ featured a single β-hairpin in the C-terminal region of the peptide (Fig. 2).[17] We initially hypothesised that the additional three amino acid residues (SPS) at the N-terminus of *Ov*-GRN$_{9–35_3s}$ might stabilise a β-hairpin at the N-terminus of the truncated analogue as well. However, secondary shift analysis suggested that the overall structure for *Ov*-GRN$_{9–35_3s}$ is similar to *Ov*-GRN$_{12–35_3s}$ (Fig. 5).

The two-dimensional NMR spectra of *Ov*-GRN$_{39–66_3s}$ were not assigned due to the presence of co-eluting fully oxidised species and the presence of broad peaks, which precluded reliable peak assignment and structural interpretation.

Bioactivity assay

The potency of peptides corresponding to the N-terminal (*Ov*-GRN$_{9–35_3s}$) and C-terminal (*Ov*-GRN$_{39–66_3s}$) regions of *Ov*-GRN-1 in driving the proliferation of a human normal fibroblast cell line (1BR.3.GN) was assessed using a real-time xCELLigence cell proliferation assay.

The N-terminal truncated analogue, *Ov*-GRN$_{9–35_3s}$, significantly enhanced fibroblast proliferation by 121% ($P < 0.0001$) at 1 μM, as shown in Fig. 6. These findings are consistent with our previous observations on *Ov*-GRN$_{12–35_3s}$, which shares the same cysteine framework (Table 1) and a comparable overall secondary structure (Fig. 5).[17,18]

Although *Ov*-GRN$_{9–35_3s}$ and *Ov*-GRN$_{12–35_3s}$ appear to have similar structures based on NMR secondary shift analysis, with the main element of the secondary structure a β-hairpin, previous work has demonstrated that the three-dimensional structure is not necessary for bioactivity of *Ov*-GRN-1 N-terminally truncated peptides.[19] Further downsizing of the peptides corresponding to the N-terminal domain of *Ov*-GRN-1 into smaller peptide fragments, representing inter-cysteine loops, showed that the seven-residue

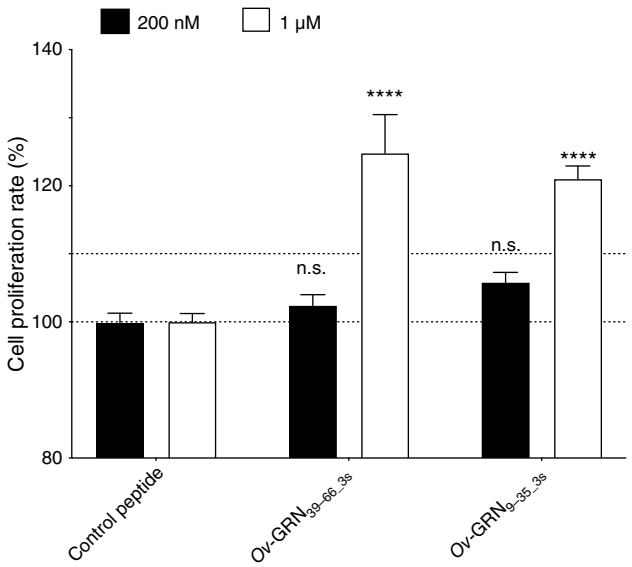


Fig. 6. Cell proliferation analysis of granulin peptides using xCELLigence technology. Fibroblast cells were treated with peptides at concentrations of 200 nM (black) and 1 μM (white). Cell index was measured after 120 h post treatment. Data represent mean ± s.e.m. of three independent experiments. Data were analysed by two-way ANOVA against peptide control (ns, not significant; ****, $P < 0.0001$).

peptide corresponding to inter-cysteine loop 2 (Table 1) promotes cell proliferation of human fibroblasts.[19]

The fraction of *Ov*-GRN$_{39–66_3s}$ analysed with NMR spectroscopy that showed no ordered structure was also analysed in the fibroblast proliferation assay. At a concentration of 1 μM, this fraction enhanced fibroblast cell proliferation (125%, $P < 0.0001$), as shown in Fig. 6. At a concentration of 1 μM, this fraction enhanced fibroblast cell proliferation (121%, $P < 0.001$), as shown in Fig. 6. These data further support the hypothesis that a well-defined 3-D structure

Downloaded from connectsci.au/ch/article-pdf/doi/10.1071/CH25079/1798680/ch25079.pdf by James Cook University user on 29 October 2026

may not be critical for the cell proliferation bioactivity of *Ov*-GRN-1 truncated analogues and that the proliferative activity is predominantly governed by specific sequence motifs rather than by a stable tertiary structure.

There are several other examples where it has been shown that a well-defined 3-D structure is not necessary for granulin bioactivity.[33–35] It has been previously shown that neither the fully oxidised nor fully reduced form of human granulin B (GRN-3) is structured in solution,[9,36] but the fully reduced form modestly induces NF-κB activation and consequently suppresses inflammation in SY-SH5Y human neuroblastoma cells.[15] Furthermore, it has been shown that the disordered form of the hGRNB modulates Aβ-induced aggregation and cytotoxicity in Alzheimer's disease, the same as the fully oxidised form.[37]

The mechanism of action of *Ov*-GRN-1 granulin peptides, and hence the receptor, has yet to be established. It is possible that upon binding to a biological target, structural changes occur that induce structural order and enhance peptide binding to the receptors.[33,34] It is also noteworthy to mention that the *Ov*-GRN$_{39–66_3s}$ peptide contains an Arg-Gly-Asp (RGD) sequence, which is the minimal integrin binding motif.[38] RGD-binding integrins such as αvβ3, αvβ5, αvβ6, αvβ8, α5β1 and αIIbβ3 are heterodimeric cell surface receptors involved in the regulation of multiple physiological processes such as cell proliferation, differentiation and apoptosis.[39] Short linear peptides mimicking the RGD sequence have been developed and used for therapeutic purposes, either as a therapeutic agent for modulation of integrin function or carrying therapeutics for treating a wide range of diseases.[39–43] The presence of the RGD sequence motif in *Ov*-GRN$_{39–66_3s}$ might be responsible for the bioactivity observed in the current study, but mutational studies would be required to confirm this hypothesis.

Conclusion

Investigating the structure-function relationships of *Ov*-GRN-1 through downsized analogues has provided significant insights into the folding and bioactivity of the granulin peptides. This study focused on the C-terminal half of the granulin domain and compared its folding, structural features and biological activity to the N-terminal half of the domain. The C-terminal analogue did not autonomously fold with three disulfide bonds into a one major conformation and showed no evidence of regular secondary structure formation, in contrast with the N-terminal analogues. In addition, the C-terminal fragment also enhanced the cell proliferation of fibroblast cells. This result suggests that fibroblast cell proliferation, induced by granulin peptides, does not appear to be dependent on having a well-defined structure. The inter-cysteine loops of the N- and C-terminal regions of *Ov*-GRN-1 have no similarity and therefore further structure–function investigations are required to determine the residues involved in the bioactivity.

Materials and methods

Peptide, synthesis, purification and characterisation

Truncated granulin peptides were synthesised on a Protein Technologies PS3 synthesiser, using 2-chlorotrityl-chloride resin. The Fmoc amino acid derivatives (Auspep, Melbourne, Vic., Australia) were sequentially coupled on the resin using a standard DIEA/HCTU protocol. Fmoc-Cysteine residues were trityl protected. Peptides were cleaved from the solid support by treatment with a mixture of TFA:TIPS:H_2O (at ratios of 95%:2.5%:2.5% v/v), followed by purging with nitrogen to evaporate TFA. Peptides were then precipitated in ice-cold diethyl ether and dissolved in 50% acetonitrile:50% H_2O containing 0.1% TFA (v/v) and subsequently lyophilised. The crude peptides were purified by reversed-phase HPLC on a Phenomenex Jupiter C18 preparative column (300 Å, 10 μm, 250 × 21.2 mm), using a gradient of 0–60% solvent B (Solvent A: 99.95% H_2O:0.05% TFA; Solvent B: 90% acetonitrile:10% H_2O containing 0.045% TFA) over 60 min. The collected fractions were characterised using a SCIEX 5800 MALDI TOF/TOF mass spectrometer (SCIEX, Foster City, CA, USA) and then lyophilised.

Disulfide bond formation

Disulfide bonds were formed as described previously.[17,18] Reduced peptide (0.1 mg mL^{-1}) was dissolved in ammonium bicarbonate buffer (0.1 M, pH 8–8.2) containing reduced glutathione (5 mM) at room temperature. To examine the effect of organic solvents on the folding properties of the peptide, up to 40% isopropanol or acetonitrile was added to the oxidation buffer. The presence of disulfide-bond species was examined by removing aliquots from the folding mixture at selected time points and analysing them with analytical RP-HPLC using a Phenomenex Jupiter 4-μm Proteo column (150 × 2.00 mm, 90 Å). When the oxidation was completed, the oxidation solution was acidified with TFA and loaded on a C_{18} preparative column (Phenomenex Jupiter 250 × 21.2 mm, 10 μm, 300 Å). with a flow rate of 6 mL min^{-1}. The separation method was as follows: a gradient of 0–50% solvent B over 50 min. Fractions were collected and the peptide mass was analysed using a SCIEX 5800 MALDI TOF/TOF spectrometer.

NMR spectroscopy

Lyophilised peptide was dissolved in 90%H_2O:10% D_2O at a concentration of ~0.2 mM. All NMR spectra were acquired on a Bruker 600-MHz AVANCE III NMR spectrometer (Bruker, Karlsruhe, Germany). 2-D ^{1}H–^{1}H TOCSY, ^{1}H–^{1}H NOESY and ^{1}H–^{1}H DQF-COSY, collected at 290 K, were used for sequence-specific assignments and structure calculations. ^{1}H–^{15}N HSQC and ^{1}H–^{13}C HSQC spectra were acquired for nitrogen and carbon chemical shifts respectively. Two-dimensional homonuclear NOESY and TOCSY spectra were acquired with a mixing time of 200 ms and a spin lock time of 80 ms respectively. All spectra were processed using Bruker *TopSpin*

Downloaded from connectsci.au/ch/article-pdf/doi/10.1071/CH25079/1798680/ch25079.pdf by James Cook University user on 29 October 2026

(ver. 3.5pl7, see https://www.bruker.com/en/products-and-solutions/mr/nmr-software/topspin.html) and assigned using the *CcpNmr* analysis program (ver. 2.1, see https://ccpn.ac.uk/software/version-2/) based on the approach described in Wüthrich.[44] The αH secondary shifts were determined by subtracting random coil ^{1}H NMR chemical shifts[32] from the experimental αH chemical shifts.

Mammalian cell culture

The human skin normal fibroblast cell line, 1BR.3.GN (ECACC 90020509), was purchased from the European Collection of Authenticated Cell Cultures (ECACC). The 1BR.3.GN fibroblasts were grown and maintained in Gibco DMEM/F12 containing Gibco antibiotic and antimycotic (1×) and Gibco GlutaMAX (1×), supplemented with Gibco foetal bovine serum (10%) (FBS) (all from ThermoFisher Scientific, Melbourne, Vic., Australia) at 37°C and CO_2 (5%). The same medium was used for all treatments in the cell proliferation assays unless specified.

Cell proliferation monitoring in real time using xCELLigence

An xCELLigence Real Time Cell Analyser – Single Plate (RTCA SP) instrument (ACEA Biosciences, San Diego, CA, USA) was used to evaluate cell proliferation as described previously.[17,18] Briefly, 1BR.3.GN cells (7500 cells/well) were seeded into a 96-well xCELLigence E-plate (ACEA Biosciences). The E-plate was placed into the xCELLigence station and incubated at 37°C with 5% CO_2 and monitored overnight (<16 h). The following day, the media was subsequently aspirated and replaced with starvation media (150 µL of DMEM/F12 media supplemented with 1× antibiotic/antimycotic, 1× GlutaMAX, 0.5% FBS) and incubated overnight. Treatments were added in fresh media (DMEM/F12 media supplemented with 1× antibiotic/antimycotic, 1× GlutaMAX, 10% FBS) to each well in a total volume of 150 µL to provide 200-nM or 1-µM final concentrations in quadruplicate. Cells treated with a 20-residue peptide from tropomyosin (EADRKYDEVARKLAMVEADL) served as the negative control peptide.[17,18] Cell proliferation was monitored every 1 h for up to 5 days. The cell index (CI) was normalised to the CI of the time-point when the treatments were added to the cells. The cell proliferation rate was calculated as the CI for the treated cells compared to the CI for peptide control cells (~120 h in culture). Cell proliferation rates were compared between treatment and control wells, and statistical analyses were conducted using two-way ANOVA followed by Holm–Šidák's correction for multiple comparisons, using *Prism* (ver. 6.02, GraphPad Software, Boston, MA, USA, see https://www.graphpad.com/features).

Supplementary material

Supplementary material is available online.

References

1 Diegelmann RF, Evans MC. Wound healing: an overview of acute, fibrotic and delayed healing. *Front Biosci* 2004; 9: 283–289. doi:10.2741/1184
2 Mutsaers SE, Bishop JE, McGrouther G, *et al.* Mechanisms of tissue repair: from wound healing to fibrosis. *Int J Biochem Cell Biol* 1997; 29: 5–17. doi:10.1016/s1357-2725(96)00115-x
3 Gomes A, Teixeira C, Ferraz R, *et al.* Wound-healing peptides for treatment of chronic diabetic foot ulcers and other infected skin injuries. *Molecules* 2017; 22: 1743. doi:10.3390/molecules22101743
4 He Z, Ong CH, Halper J, *et al.* Progranulin is a mediator of the wound response. *Nat Med* 2003; 9: 225–229. doi:10.1038/nm816
5 He Z, Bateman A. Progranulin (granulin-epithelin precursor, PC-cell-derived growth factor, acrogranin) mediates tissue repair and tumorigenesis. *J Mol Med* 2003; 81: 600–612. doi:10.1007/s00109-003-0474-3
6 Palfree RG, Bennett H, Bateman A. The evolution of the secreted regulatory protein progranulin. *PLoS ONE* 2015; 10: 0133749. doi:10.1371/journal.pone.0133749
7 De Muynck L, Van Damme P. Cellular effects of progranulin in health and disease. *J Mol Neurosci* 2011; 45: 549–560. doi:10.1007/s12031-011-9553-z
8 Jian J, Konopka J, Liu C. Insights into the role of progranulin in immunity, infection, and inflammation. *J Leukoc Biol* 2013; 93: 199–208. doi:10.1189/jlb.0812429
9 Tolkatchev D, Malik S, Vinogradova A, *et al.* Structure dissection of human progranulin identifies well-folded granulin/epithelin modules with unique functional activities. *Protein Sci* 2008; 17: 711–724. doi:10.1110/ps.073295308
10 Dastpeyman M, Smout MJ, Wilson D, *et al.* Folding of granulin domains. *Pept Sci* 2018; 110: e24062. doi:10.1002/pep2.24062
11 Vranken WF, James S, Bennett HP, *et al.* Solution structures of a 30-residue amino-terminal domain of the carp granulin-1 protein and its amino-terminally truncated 3-30 subfragment: implications for the conformational stability of the stack of two beta-hairpins. *Proteins* 2002; 47: 14–24.
12 Wang P, Chitramuthu B, Bateman A, *et al.* Structure dissection of zebrafish progranulins identifies a well-folded granulin/epithelin module protein with pro-cell survival activities. *Protein Sci* 2018; 27: 1476–1490. doi:10.1002/pro.3441
13 Smout MJ, Mulvenna JP, Jones MK, *et al.* Expression, refolding and purification of Ov-GRN-1, a granulin-like growth factor from the carcinogenic liver fluke, that causes proliferation of mammalian host cells. *Protein Expr Purif* 2011; 79: 263–270. doi:10.1016/j.pep.2011.06.018
14 Hrabal R, Chen Z, James S, *et al.* The hairpin stack fold, a novel protein architecture for a new family of protein growth factors. *Nat Struct Biol* 1996; 3: 747–752. doi:10.1038/nsb0996-747
15 Ghag G, Wolf LM, Reed RG, *et al.* Fully reduced granulin-B is intrinsically disordered and displays concentration-dependent dynamics. *Protein Eng Des Sel* 2016; 29: 177–186. doi:10.1093/protein/gzw005
16 Smout MJ, Laha T, Mulvenna J, *et al.* A granulin-like growth factor secreted by the carcinogenic liver fluke, *Opisthorchis viverrini*, promotes proliferation of host cells. *PLoS Pathog* 2009; 5: 1000611. doi:10.1371/journal.ppat.1000611
17 Bansal PS, Smout MJ, Wilson D, *et al.* Development of a potent wound healing agent based on the liver fluke granulin structural fold. *J Med Chem* 2017; 60: 4258–66. doi:10.1021/acs.jmedchem.7b00047
18 Dastpeyman M, Bansal PS, Wilson D, *et al.* Structural variants of a liver fluke derived granulin peptide potently stimulate wound healing. *J Med Chem* 2018; 61: 8746–8753. doi:10.1021/acs.jmedchem.8b00898
19 Takjoo R, Wilson DT, Bansal PS, *et al.* Identification of an inter-cysteine loop potentially involved in the activity of *Opisthorchis viverrini*-granulin-1. *Explor Drug Sci* 2023; 1: 172–179. doi:10.37349/eds.2023.00012
20 Dastpeyman M. Structure–function relationships of disulfide-rich peptides. PhD thesis. Cairns, Qld, Australia: James Cook University; 2019. doi:10.25903/5ea659714d9ab
21 Mamathambika BS, Bardwell JC. Disulfide-linked protein folding pathways. *Annu Rev Cell Dev Biol* 2008; 24: 211–235. doi:10.1146/annurev.cellbio.24.110707.175333

Downloaded from connectsci.au/ch/article-pdf/doi/10.1071/CH25079/1798680/ch25079.pdf by James Cook University user on 29 October 2026

22 Chang JY. Diverse pathways of oxidative folding of disulfide proteins: underlying causes and folding models. *Biochemistry* 2011; 50: 3414–3431. doi:10.1021/bi200131j

23 Clark RJ, Jensen J, Nevin ST, *et al.* The engineering of an orally active conotoxin for the treatment of neuropathic pain. *Angew Chem Int Ed Engl* 2010; 49: 6545–6548. doi:10.1002/anie.201000620

24 Góngora-Benítez M, Tulla-Puche J, Paradís-Bas M, *et al.* Optimized Fmoc solid-phase synthesis of the cysteine-rich peptide linaclotide. *Biopolymers* 2011; 96: 69–80. doi:10.1002/bip.21480

25 Metanis N, Hilvert D. Strategic use of non-native diselenide bridges to steer oxidative protein folding. *Angew Chem Int Ed Engl* 2012; 51: 5585–5588. doi:10.1002/anie.201109129

26 Koradi R, Billeter M, Wuthrich K. *MOLMOL*: a program for display and analysis of macromolecular structures. *J Mol Graph* 1996; 14: 51–55. doi:10.1016/0263-7855(96)00009-4

27 Belcourt DR, Lazure C, Bennett H. Isolation and primary structure of the three major forms of granulin-like peptides from hematopoietic tissues of a teleost fish (*Cyprinus carpio*). *J Biol Chem* 1993; 268: 9230–9237.

28 Sasaki T, Feng ZP, Scott R, *et al.* Synthesis, bioactivity, and cloning of the L-type calcium channel blocker omega-conotoxin TxVII. *Biochemistry* 1999; 38: 12876–12884. doi:10.1021/bi990731f

29 DeLa Cruz R, Whitby FG, Buczek O, *et al.* Detergent-assisted oxidative folding of delta-conotoxins. *J Pept Res* 2003; 61: 202–212. doi:10.1034/j.1399-3011.2003.00048.x

30 Daly NL, Love S, Alewood PF, *et al.* Chemical synthesis and folding pathways of large cyclic polypeptides: studies of the cystine knot polypeptide kalata B1. *Biochemistry* 1999; 38: 10606–10614. doi:10.1021/bi990605b

31 Rehm T, Huber R, Holak TA. Application of NMR in structural proteomics: screening for proteins amenable to structural analysis. *Structure* 2002; 10: 1613–1618. doi:10.1016/s0969-2126(02)00894-8

32 Wishart DS, Bigam CG, Yao J, *et al.* ^{1}H, ^{13}C and ^{15}N chemical shift referencing in biomolecular NMR. *J Biomol NMR* 1995; 6: 135–140. doi:10.1007/BF00211777

33 Uversky VN. A decade and a half of protein intrinsic disorder: biology still waits for physics. *Protein Sci* 2013; 22: 693–724. doi:10.1002/pro.2261

34 Dyson HJ, Wright PE. Intrinsically unstructured proteins and their functions. *Nat Rev Mol Cell Biol* 2005; 6: 197–208. doi:10.1038/nrm1589

35 Dunker AK, Silman I, Uversky VN, *et al.* Function and structure of inherently disordered proteins. *Curr Opin Struct Biol* 2008; 18: 756–64. doi:10.1016/j.sbi.2008.10.002

36 Ghag G, Holler CJ, Taylor G, *et al.* Disulfide bonds and disorder in granulin-3: an unusual handshake between structural stability and plasticity. *Protein Sci* 2017; 26: 1759–1772. doi:10.1002/pro.3212

37 Bhopatkar AA, Ghag G, Wolf LM, *et al.* Cysteine-rich granulin-3 rapidly promotes amyloid-β fibrils in both redox states. *Biochem J* 2019; 476: 859–873. doi:10.1042/BCJ20180916

38 Wohlrab S, Müller S, Schmidt A, *et al.* Cell adhesion and proliferation on RGD-modified recombinant spider silk proteins. *Biomaterials* 2012; 33: 6650–6659. doi:10.1016/j.biomaterials.2012.05.069

39 Kapp TG, Rechenmacher F, Neubauer S, *et al.* A comprehensive evaluation of the activity and selectivity profile of ligands for RGD-binding integrins. *Sci Rep* 2017; 7: 39805. doi:10.1038/srep39805

40 Auzzas L, Zanardi F, Battistini L, *et al.* Targeting alphavbeta3 integrin: design and applications of mono- and multifunctional RGD-based peptides and semipeptides. *Curr Med Chem* 2010; 17: 1255–1299. doi:10.2174/092986710790936301

41 Marelli UK, Rechenmacher F, Sobahi TR, *et al.* Tumor targeting via integrin ligands. *Front Oncol* 2013; 3: 222. doi:10.3389/fonc.2013.00222

42 Arosio D, Manzoni L, Corno C, *et al.* Integrin-targeted peptide- and peptidomimetic-drug conjugates for the treatment of tumors. *Recent Pat Anticancer Drug Discov* 2017; 12: 148–168. doi:10.2174/1574892812666170203151930

43 Majumder P. Integrin-mediated delivery of drugs and nucleic acids for anti-angiogenic cancer therapy: current landscape and remaining challenges. *Bioengineering* 2018; 5: 76. doi:10.3390/bioengineering5040076

44 Wüthrich K. NMR studies of structure and function of biological macromolecules (Nobel Lecture). *J Biomol NMR* 2003; 27: 13–39. doi:10.1023/a:1024733922459

Data availability. The data are presented in the manuscript or are available upon request.

Conflicts of interest. The authors declare that they have no conflicts of interest.

Declaration of funding. This work was supported by an AITHM PhD scholarship to M. Dastpeyman. The James Cook University NMR facility was partially funded by the Australian Research Council (N. L. Daly, A. Loukas) (LE160100218). M. J. Smout and A. Loukas were supported by the National Cancer Institute, National Institutes of Health, award R01 CA164719.

Author affiliations

[A]Australian Institute of Tropical Health and Medicine, James Cook University, Cairns, Qld, Australia.

[B]Department of Biochemistry and Molecular Biology, Immunity Program, Biomedicine Discovery Institute, Monash University, Clayton, Vic., Australia.

Downloaded from connectsci.au/ch/article-pdf/doi/10.1071/CH25079/1798680/ch25079.pdf by James Cook University user on 29 October 2026